# Adiabatic theory of one-dimensional curved polariton waveguides

D. A. Zezyulin[1,*] and I. A. Shelykh[1,2,3]

[1]*School of Physics and Engineering, ITMO University, St. Petersburg 197101, Russia*

[2]*Abrikosov Center for Theoretical Physics, MIPT, Dolgoprudny, Moscow Region 141701, Russia*

[3]*Science Institute, University of Iceland, Dunhagi 3, IS-107, Reykjavik, Iceland*

(Received 9 January 2023; revised 25 April 2023; accepted 28 April 2023; published 11 May 2023)

We construct a general theory of adiabatic propagation of spinor exciton polaritons in waveguides of arbitrary shape, accounting for the effects of TE-TM splitting in linear polarizations and Zeeman splitting in circular polarizations. The developed theory is applied for the description of waveguides of periodically curved shape. We show that in this geometry the periodic rotation of the effective in-plane magnetic field produced by TE-TM interaction results in a nontrivial band-gap structure, which can be additionally tuned by application of an external magnetic field. It is also demonstrated that spin-dependent interactions between polaritons lead to the formation of stable gap solitons.

DOI: 10.1103/PhysRevB.107.205303

## I. INTRODUCTION

If characteristic energy of the light-matter interaction exceeds the values of the broadenings related to the losses in the system, the regime of strong light-matter coupling is established, and polaritons, i.e., hybrid half-light–half-matter elementary excitations, are formed. In particular, exciton polaritons emerge in the regime of the strong coupling between a photonic mode of a planar semiconductor microcavity and an exciton in a quantum well (QW) brought in resonance with it. They possess a set of remarkable properties, which allow polaritonic systems to serve as a convenient playground for study of collective nonlinear phenomena at elevated temperatures [1]. From their photonic component polaritons get extremely small effective mass (about $10^{-5}$ of the mass of free electrons) and macroscopically large coherence length [2], while the presence of an excitonic component enables efficient polariton-polariton interactions [3–5] and leads to the sensitivity of the polariton systems to external electric [6–8] and magnetic [9–11] fields.

An important property of cavity polaritons is their spin (or pseudospin) [12], inherited from the spins of QW excitons and cavity photons. Similar to photons, polaritons have two possible spin projections on the structure growth axis corresponding to the two opposite circular polarizations, which can be mixed by effective magnetic fields of various origin. Real magnetic field applied along the structure growth axis and acting on the excitonic component splits in energy the polariton states with opposite circular polarizations, while TE-TM splitting of the photonic modes of a planar resonator couples these states to each other via a $k$-dependent term, thus playing a role of an effective spin-orbit interaction [12]. Importantly, polariton-polariton interactions are also spin dependent, as they stem from the interactions of excitonic components which are dominated by the exchange term [13]. This leads to the fact that polaritons of the same circular polarization interact orders of magnitude stronger than polaritons with opposite circular polarizations [3].

Remarkable tunability of cavity polaritons allows one to engineer their spatial confinement in a variety of experimental geometries, ranging from individual micropillars [14–17] to systems of several coupled pillars forming so-called polariton molecules [18,19] or periodically arranged arrays of the pillars forming polariton superlattices [20–24]. Periodically structured polaritons represent particular interest as they can feature nontrivial band structures that enable topological phases and can be used to implement polariton topological insulators; see Ref. [25] for a review. Combined effect of periodicity and effective nonlinearity enables formation of polariton gap [26–30] and gap-stripe solitons [31], as well as topological edge solitons [32]. On the other hand, realization of quasi-one-dimensional (1D) geometries, where the motion of the polaritons is restricted to individual waveguides [7,33], rings [34–36], or systems of coupled waveguides [37,38], represents particular interest from the point of view of the applications of polaritonics, as they can form the basis for classical [39–41] and quantum [42,43] polaritonic circuits.

The current state of technology allows routine production of quasi-1D polariton waveguides of arbitrary shape, including ones with periodically modulated curvature. Creation of the general theory of the polariton propagation in these structures, which includes polarization dynamics and polariton-polariton interactions, is the goal of the present paper. Its content is organized as follows. In Sec. II we introduce the model of a curved waveguide and derive the effective equations. In Sec. III we provide a more detailed discussion of two particular examples of waveguides with periodic curvature and illustrate nontrivial band-gap structures that result from the effective periodicity. Section IV presents a discussion of gap solitons forming in curved waveguides. Section V concludes the paper.

*d.zezyulin@gmail.com

 

## II. MODEL

Let us suppose that the shape of a waveguide in $(x, y)$ plane is given parametrically as $x = x(\xi)$, $y = y(\xi)$, where variable $\xi$ is used as a parameter. The presence of the in-plane spatial confinement results in the strong nonequivalency of the states polarized normally and tangentially to the waveguide, which leads to the appearance of a local effective magnetic field, acting on a polariton pseudospin and directed tangentially to the waveguide. Although one can safely assume that in the case of a narrow waveguide of a constant width the absolute value of this field remains constant (see the Appendix for further details), its direction changes along the curved waveguide and, as we demonstrate below, this has a crucial effect on polariton dynamics.

The components of the effective magnetic field $\Omega_{x,y}$ produced by TE-TM interaction are proportional to the components of the unit vector tangential to a waveguide $\tau_{x,y}$ and thus read

$$\Omega_x = \Omega_0 \tau_x = \frac{\Omega_0 x'(\xi)}{\sqrt{x'(\xi)^2 + y'(\xi)^2}}, \tag{1}$$

$$\Omega_y = \Omega_0 \tau_y = \frac{\Omega_0 y'(\xi)}{\sqrt{x'(\xi)^2 + y'(\xi)^2}}, \tag{2}$$

where primes correspond to derivatives, and

$$\Omega_0 \approx \frac{\hbar^2}{4d^2}\left(\frac{1}{m_l} - \frac{1}{m_t}\right). \tag{3}$$

In the above equation, $m_l$ and $m_t$ stand for the effective longitudinal and transverse masses of 2D polaritons and $d$ is an effective width of a polariton channel [44]. As it was already mentioned, the presence of the field $\mathbf{\Omega}$ splits in energy the modes polarized normally and tangentially to a waveguide. Additional splitting in circular polarizations, denoted by $\Delta_z$, can be induced by application of an external magnetic field perpendicular to a cavity interface.

Let us introduce the coordinate $\ell$ along the waveguide, $\ell = \int_0^\xi \sqrt{x'(\eta)^2 + y'(\eta)^2} d\eta$. In the adiabatic approximation, the effective 1D Hamiltonian governing the dynamics of the spinor wavefunction of polaritons can be then represented in the following form (see Appendix for corresponding derivation):

$$\hat{H} = \begin{pmatrix} -\frac{\hbar^2}{2m_{\text{eff}}}\frac{d^2}{d\ell^2} + \frac{\Delta_z}{2} & \Omega_- \\ \Omega_+ & -\frac{\hbar^2}{2m_{\text{eff}}}\frac{d^2}{d\ell^2} - \frac{\Delta_z}{2} \end{pmatrix}, \tag{4}$$

where

$$\Omega_\pm = \Omega(\ell) = \Omega_0(\tau_x \pm i\tau_y)^2 \tag{5}$$

and $m_{\text{eff}}$ is the effective mass. We particularly note that Hamiltonian $\hat{H}$ assumes the conservative dynamics and neglects the polariton losses whose effect is left for future studies.

The physical meaning of the above Hamiltonian is pretty clear: it describes a motion of a one-dimensional spinor particle affected by a constant $z$-directed magnetic field and in-plane magnetic field whose direction changes along the way, being always tangential to the waveguide.

In what follows, we will work with the effective Hamiltonian rewritten in the dimensionless form. To this end, we introduce the unit length $\lambda_0$ and the unit energy $\varepsilon_0 \equiv \hbar^2/(2m_{\text{eff}}\lambda_0^2)$ and then rescale the variables of (4) as $\ell \to \lambda_0 \ell$ and $\Delta_z \to \varepsilon_0 \Delta_z$. Additionally, we rescale time as $t \to (\hbar/\varepsilon_0)t$. To estimate the relevant length unit, we refer to recent experiments with exciton-polariton routing devices [38], where quasi-one-dimensional waveguides having thickness of about 2 μm and total length of ∼100 μm were fabricated. It is therefore reasonable to assume that the unit length $\lambda_0$ corresponds to 1 μm. Then, assuming that the effective mass $m_{\text{eff}}$ is about $10^{-5}$ of the free electron mass, we obtain that the unit energy $\varepsilon_0$ is about 3.8 meV and the time unit $\hbar/\varepsilon_0$ is approximately equal to 0.2 ps. While our theoretical study disregards the effect of polariton losses, in order to interpret the obtained time unit we note that in the mentioned experiment [38] the polariton population dissipated after approximately 30 ps. Supplementing the obtained dimensionless Hamiltonian with the interaction terms [45], we obtain the following nonlinear evolution problem that governs the dynamics of the spinor wavefunction $(\Psi_1, \Psi_2)$:

$$i\frac{\partial \Psi_1}{\partial t} = -\frac{\partial^2 \Psi_1}{\partial \ell^2} + \frac{\Delta_z}{2}\Psi_1 + \Omega_-(\ell)\Psi_2 + (|\Psi_1|^2 + \sigma|\Psi_2|^2)\Psi_1, \tag{6}$$

$$i\frac{\partial \Psi_2}{\partial t} = -\frac{\partial^2 \Psi_2}{\partial \ell^2} - \frac{\Delta_z}{2}\Psi_2 + \Omega_+(\ell)\Psi_1 + (|\Psi_2|^2 + \sigma|\Psi_1|^2)\Psi_2. \tag{7}$$

Small negative coefficient $\sigma$ takes into account weak attraction between polaritons of opposite polarizations (in our numerical calculations the value $\sigma = -0.05$ was used).

## III. BAND STRUCTURE IN PERIODIC WAVEGUIDES

In what follows, we focus on the situation when the shape of the curved waveguide can be described by function $y(x)$; see Fig. 1(a) for a schematics of the assumed geometry. Then the effective field, as a function of the arc length $\ell$, can be computed as $\Omega_\pm(\ell) = \Omega_0 \exp\{\pm 2i \arctan(dy/dx)\}$, where the derivative $dy/dx$ should be expressed as a function of $\ell$. In our further consideration we focus on the case of periodically curved waveguides.

As a first analytically tractable example we consider the situation when the waveguide is composed of a periodic chain of touching half circles of a radius $R$. In terms of coordinates $x$ and $y$, the unit cell of the resulting periodic structure is given as $y(x) = \sqrt{R^2 - (x-R)^2}$ for $x \in [0, 2R]$ (the upper half circle) and $y(x) = -\sqrt{R^2 - (x-3R)^2}$ for $x \in [2R, 4R]$ (the lower half circle). In terms of the arc length $\ell$, the unit cell corresponds to the interval $\ell \in [0, L]$, where $L = 2\pi R$ is the period of the structure. The first half period $\ell \in [0, \pi R]$ corresponds to the first half circle, where $x(\ell) = R[1 - \cos(\ell/R)]$ and $y(\ell) = R\sin(\ell/R)$, and the second half period $\ell \in [\pi R, 2\pi R]$ corresponds to the second half circle, where we have parametrization $x(\ell) = R[3 + \cos(\ell/R)]$ and $y(\ell) = R\sin(\ell/R)$ and the rest of the waveguide is obtained by the periodic repetition of the unit cell. Performing straightforward calculations, we obtain that within the unit cell the

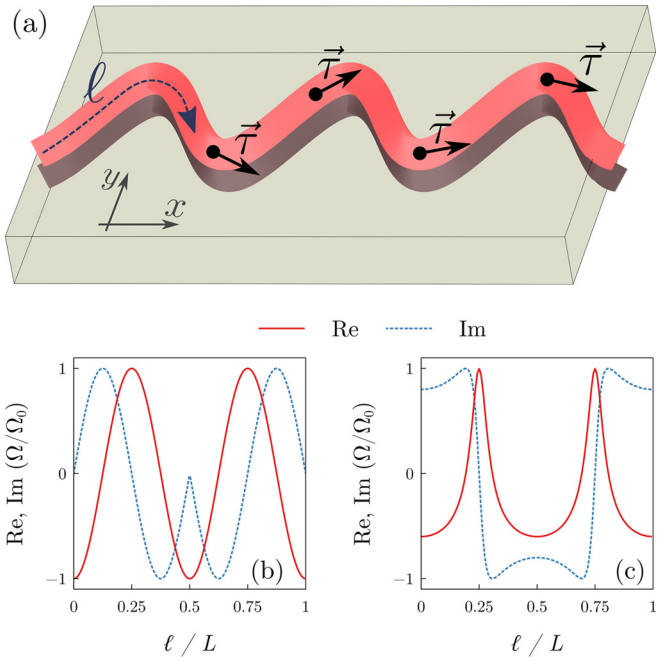


FIG. 1. (a) Schematic representation of the considered geometry of a 1D polariton waveguide etched in planar semiconductor microcavity. The arc length $\ell$ measures the distance along the waveguide. Direction of the in-plane tangential unit vector $\vec{\tau} = (\tau_x, \tau_y)$ changes along the waveguide and leads to emergence of an effective space-dependent field for the spinor polariton wavefunction. (b),(c) Real and imaginary parts of the $L$-periodic effective potentials $\Omega(\ell)$ for a waveguide composed of a chain of touching half circles (b) and a sine-shaped waveguide (c).

resulting potential reads $\Omega_{\pm}(\ell) = -\Omega_0 \exp\{\mp 2i\ell\, \mathrm{sgn}\,(\pi R - \ell)/R\}$. The shape of the resulting dependency is illustrated in Fig. 1(b). While the obtained dependence is rather simple, its imaginary part is not a smooth function: it has a cusp exactly at the center of the unit cell $\ell = \pi R$, where the two half circles touch.

As a second example, which results in a smooth periodic potential (which is therefore better suited for the numerical analysis), we consider a sine-shaped waveguide $y(x) = V_0 \sin x$. Then the arc length along the waveguide is given by the incomplete elliptic integral of the second kind [46]: $\ell(x) = \sqrt{1+V_0^2}\,\mathcal{E}(\sin x, m)$, where $m = V_0^2/(1+V_0^2)$. To the best of our knowledge, there is neither a commonly used special function nor a closed-form expression that allows one to invert the incomplete elliptic integral of the second kind, i.e., to express $x$ and $y$ through $\ell$ in our case. In the meantime, there exists a simple iterative numerical procedure for inversion of the incomplete elliptic integral of the second kind [47]. Using this procedure, one can easily obtain the dependence $\Omega(\ell)$; see Fig. 1(c) for a representative example. The resulting 1D Hamiltonian $\hat{H}$ defined by (4) becomes effectively periodic with the spatial period in $\ell$ given as $L = 4\mathcal{E}(m)$, where $\mathcal{E}(m)$ is the complete elliptic integral of the second kind.

The periodic nature of the resulting system suggests looking at the band structure, which can be presented in the form of the dependencies of the energy $E$ versus Bloch quasimomentum $k$, which, without loss of generality, can be assumed to belong to the Brillouin zone $[-\pi/L, \pi/L)$, where $L$ is the period. For sinusoidal waveguide the result computed for system (6)–(7) with omitted nonlinear terms $(|\Psi_{1,2}|^2 + \sigma|\Psi_{2,1}|^2)\Psi_{1,2}$ is shown in Fig. 2. We have focused on the transformation of the spectral structure subject to the increase of the external magnetic field, which is characterized by the Zeeman splitting coefficient $\Delta_z$. As one can see, the periodic curvature of a waveguide results in a nontrivial band-gap structure as the effective periodic potential $\Omega(\ell)$ opens finite gaps even in the absence of the external magnetic field ($\Delta_z = 0$). The increase of $\Delta_z$ leads to a transformation of the band-gap structure. In particular, it leads to the anticrossing of the bands touching at $k = 0$ and related shift of the band minima and maxima to $k \neq 0$. Dispersion curves having two degenerate extrema at $k = \pm k_0 \neq 0$ can be, in particular, relevant for the observation of the so-called stripe phase characterized by spinor wavefunctions carrying a more complex internal structure; see, e.g., Refs. [48–52] and [31] for discussion of stripe phase and stripe solitons in spin-orbit coupled atomic and polariton condensates, respectively.

## IV. GAP SOLITONS

The presence of finite gaps in the band-gap structure suggests that when the repulsive interactions between the polaritons of the same circular polarization are taken into account, the waveguide can support formation of polariton gap solitons [22,27–29,31,53,54]. These localized states can be found using the substitution $\Psi_{1,2}(t, \ell) = e^{-i\mu t}\psi_{1,2}(\ell)$, where stationary wavefunctions $\psi_{1,2}(\ell)$ satisfy zero boundary conditions at $\ell \to \infty$ and $\ell \to -\infty$ and $\mu$ characterizes the chemical potential of the polariton condensate. The numerical study indicates that the system supports a variety of solitons which form continuous families, i.e., can be parametrized by the continuous change of the chemical potential $\mu$ within the energy spectrum band gap. To describe the found solitons, we introduce the polariton density integral $N = \int_{-\infty}^{\infty}(|\psi_1|^2 + |\psi_2|^2)d\ell$, which characterizes the squared norm of the solution. In Fig. 3(a) we illustrate the family of fundamental (simplest) gap solitons as a dependence $N$ on $\mu$. The soliton family detaches from the left edge of the band gap, where the soliton norm vanishes: $N \to 0$. In this limit, small-amplitude solitons transform to a linear Bloch wave. As the chemical potential increases towards the right gap edge, the total norm $N$ grows monotonously. To quantify the degree of the soliton localization, we introduce an additional dimensionless characteristic $n_{99}$, which amounts to the number of spatial periods where 99% of quasiparticles are confined. The dependence $n_{99}$ on $\mu$ is also plotted in Fig. 3(a). It demonstrates nonmonotonic behavior approaching its minimal values in the center of the gap. In this regime the solitons are most localized and almost all energy can be trapped in the segment of waveguide composed of approximately from five to ten unit cells. At the same time, the quantity $n_{99}$ becomes extremely large near the edges of the gap, which means that the corresponding solitons are very broad and relatively poorly localized. Examples of spatial profiles of solitons having different amplitudes and degrees of localization are shown in Fig. 3(b). (The threshold of 99% is chosen as a representative percentage; any other sufficiently

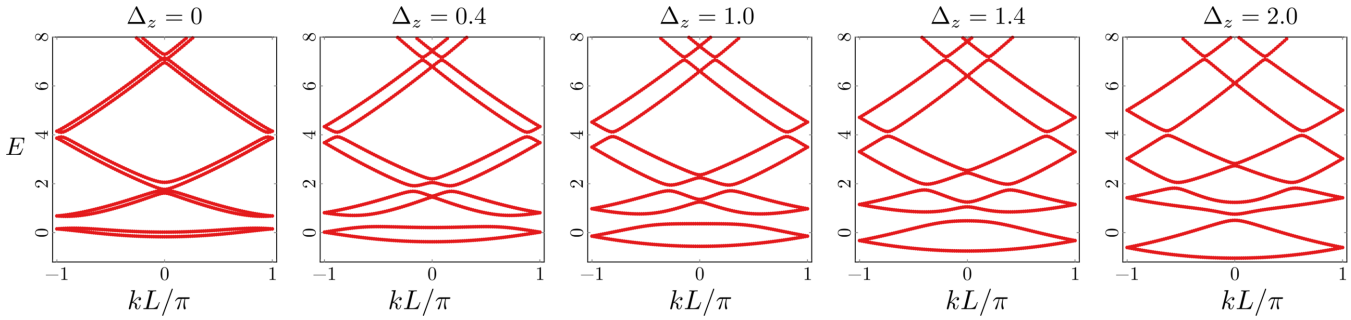


FIG. 2. Transformation of the band-gap structure for the sine-shaped waveguide under the fixed TE-TM splitting coefficient $\Omega_0 = 0.45$ and increasing strength of the external magnetic field $\Delta_z$. Here the Bloch quasimomentum $k$ varies within the reduced Brillouin zone $[-\pi/L, \pi/L)$, where $L$ is the spatial period of the structure. The periodic curvature results in a nontrivial band-gap structure. Finite band gaps are present even in the absence of the external magnetic field ($\Delta_z = 0$). The increase of $\Delta_z$ leads to the anticrossings of the bands touching at $k = 0$ and related shift of the band minima and maxima to $k \neq 0$.

large threshold, such as 95%, 90%, etc., naturally yields a similar picture.)

It is known that gap solitons and, in particular, those in systems dominated by repulsive nonlinearities can be be prone to dynamical instabilities [55–58]. In the meantime, using the dynamical simulations, we found that the family of fundamental gap solitons presented in Fig. 3(a) contains stable solutions which can robustly preserve the steady shape for the indefinite simulation time (much larger than typical polariton lifetimes), even if the initial profiles are perturbed by a small-amplitude random noise. An example of such stable dynamics is presented in Figs. 3(c) and 3(d). At the same time, more complex solitons can develop dynamical instabilities which eventually lead to their delocalization. The corresponding example is shown in Figs. 3(e) and 3(f). While unavoidable losses limit the soliton's lifetime in any real-world waveguide, the dynamics shown in Figs. 3(e) and 3(f) indicates that the soliton instabilities can be strong enough to manifest themselves at timescales comparable to the polariton's lifetime (for chosen time and length units, the dimensionless time $t = 150$ corresponds to approximately 30 ps).

## V. CONCLUSION

In conclusion, we constructed a theory of the propagation of cavity polaritons in narrow quasi-1D waveguides of arbitrary shape and applied it to the case of periodically curved waveguides. We demonstrated that the periodic rotation of an effective in-plane magnetic field produced by TE-TM splitting in linear polarizations leads to the formation of nontrivial band structure. The shape of the bands, the band gaps, and the positions of the band extrema can be tuned by application of an external magnetic field. In the nonlinear regime the system supports formation of dynamically stable gap solitons.

While our study has been limited by the conservative approximation, it is well known that losses can play an important role in the polariton propagation. A more detailed study of this issue in an important subject for future work. General theory of curved waveguides presented herein naturally call for future studies where waveguides with aperiodic curvature can also be considered.

## ACKNOWLEDGMENTS

This work was supported by the Ministry of Science and Higher Education of Russian Federation, goszadanie No. 2019-1246. I.A.S. acknowledges support from Icelandic Research Fund (Rannis), Project No. 163082-051.

## APPENDIX: DERIVATION OF THE 1D ADIABATIC HAMILTONIAN

The two-dimensional Hamiltonian of a polariton moving inside a waveguide defined by a confining potential $U(x, y)$ is [45]

$$\hat{H}_{2D} = \begin{pmatrix} -\frac{\hbar^2}{2m_{\rm eff}}\left(\frac{\partial^2}{\partial x^2} + \frac{\partial^2}{\partial y^2}\right) + \frac{\Delta_z}{2} + U(x,y) & \beta\left(\frac{\partial}{\partial y} + i\frac{\partial}{\partial x}\right)^2 \\ \beta\left(\frac{\partial}{\partial y} - i\frac{\partial}{\partial x}\right)^2 & -\frac{\hbar^2}{2m_{\rm eff}}\left(\frac{\partial^2}{\partial x^2} + \frac{\partial^2}{\partial y^2}\right) - \frac{\Delta_z}{2} + U(x,y) \end{pmatrix}, \tag{A1}$$

where

$$\beta = \frac{\hbar^2}{4}\left(\frac{1}{m_l} - \frac{1}{m_t}\right). \tag{A2}$$

Let us introduce in each point of a waveguide local coordinate system with axis $\ell$ directed tangential to it and $n$ normal to it. The elementary lengths $d\ell$ and $dn$ read

$$d\ell = \tau_x(\ell)dx + \tau_y(\ell)dy, \tag{A3}$$

$$dn = -\tau_y(\ell)dx + \tau_x(\ell)dy, \tag{A4}$$

where $\tau_{x,y}$ are components of the unit vector tangential to the waveguide at a given point characterized by coordinate $\ell$ along the waveguide.

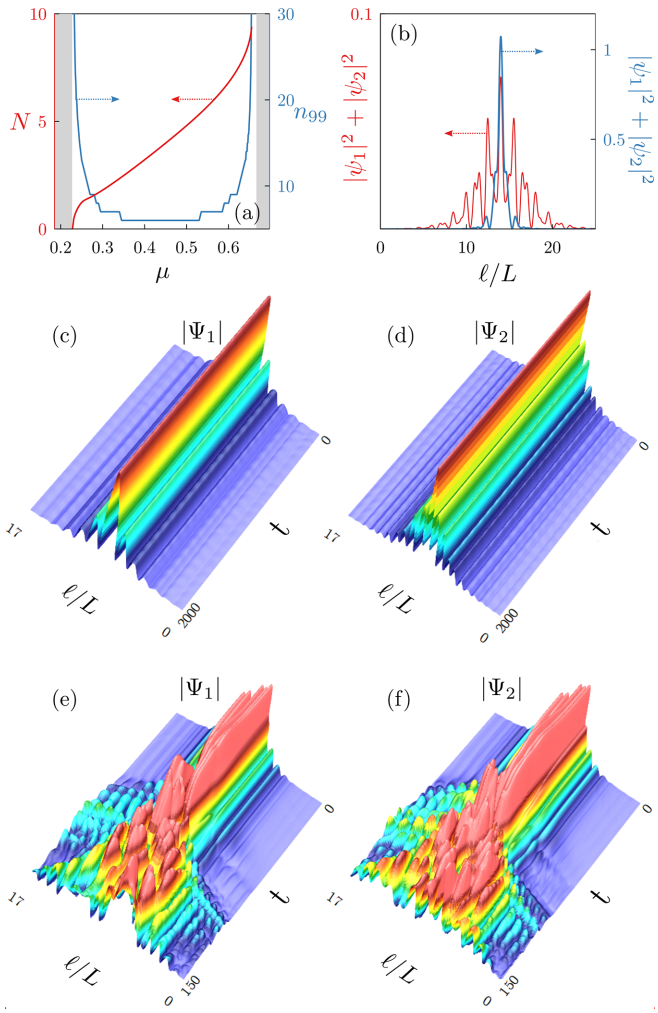


FIG. 3. (a) Gap solitons norm $N$ and the localization measure $n_{99}$ as functions of chemical potential $\mu$ for a family of fundamental gap solitons in the first finite gap. Here the coefficient of TE-TM splitting $\Omega_0 = 0.4$ and amplitude of the Zeeman splitting $\Delta_z = 0.3$. Shaded regions correspond to the values of $\mu$ that belong to spectral bands. (b) Example of a broad soliton near the left edge of the gap (specifically, at $\mu = 0.24$) and a strongly localized soliton in the center of the gap at $\mu = 0.5$. (c),(d) Stable dynamics of the gap soliton with chemical potential $\mu = 0.29$. Initial conditions correspond to the stationary wavefunctions perturbed with a random noise whose amplitude is about 2% of the soliton's amplitude. (e),(f) Example of unstable evolution of a gap soliton of more complex shape corresponding to $\Omega_0 = 0.4$, $\mu = 0.4$, and $\Delta_z = 0.009$.

We can now write down

$$\frac{\partial}{\partial x} = \frac{\partial \ell}{\partial x}\frac{\partial}{\partial \ell} + \frac{\partial n}{\partial x}\frac{\partial}{\partial n} = \tau_x \frac{\partial}{\partial \ell} - \tau_y \frac{\partial}{\partial n}, \tag{A5}$$

$$\frac{\partial}{\partial y} = \frac{\partial \ell}{\partial y}\frac{\partial}{\partial \ell} + \frac{\partial n}{\partial y}\frac{\partial}{\partial n} = \tau_y \frac{\partial}{\partial \ell} + \tau_x \frac{\partial}{\partial n}, \tag{A6}$$

$$\frac{\partial}{\partial y} \pm i\frac{\partial}{\partial x} = \pm i\tau_\mp \frac{\partial}{\partial \ell} + \tau_\mp \frac{\partial}{\partial n}, \tag{A7}$$

where

$$\tau_\pm = \tau_x \pm i\tau_y. \tag{A8}$$

We thus have

$$\frac{\partial^2}{\partial x^2} + \frac{\partial^2}{\partial y^2} = \frac{\partial^2}{\partial \ell^2} + \frac{\partial^2}{\partial n^2} + \left(\tau_y \frac{\partial \tau_x}{\partial \ell} - \tau_x \frac{\partial \tau_y}{\partial \ell}\right)\frac{\partial}{\partial n}, \tag{A9}$$

where we used that

$$\tau_x^2 + \tau_y^2 = 1. \tag{A10}$$

Similarly

$$\left(\frac{\partial}{\partial y} \pm i\frac{\partial}{\partial x}\right)^2 = \tau_\mp^2 \frac{\partial^2}{\partial n^2} - \tau_\mp \frac{\partial}{\partial \ell}\tau_\mp \frac{\partial}{\partial \ell} \pm i\tau_\mp \left(\tau_\mp \frac{\partial}{\partial \ell} + \frac{\partial}{\partial \ell}\tau_\mp\right)\frac{\partial}{\partial n}. \tag{A11}$$

Let us now suggest that the confining potential locally depends on the transverse coordinate $n$ only and use adiabatic approximation for the spinor wavefunction $\Psi(x, y)$ representing it as

$$\Psi(x, y) = \psi(\ell)\phi(n), \tag{A12}$$

where the part $\psi(\ell)$ describes the propagation of the polaritons along the waveguide and $\phi(n)$ corresponds to their 1D lateral confinement and can be taken real. This approximation holds if an effective thickness of a waveguide $d$ is much less than its local curvature $R$, which for a parametrically given curve is given by

$$R = \frac{[x'(\xi)^2 + y'(\xi)^2]^{3/2}}{|x'(\xi)y''(\xi) - y'(\xi)x''(\xi)|}. \tag{A13}$$

Multiplying the Schrödinger equation $\hat{H}_{2D}\Psi = E\Psi$ by $\phi(n)$ and integrating by $n$ from $-\infty$ to $+\infty$, one gets for the dynamics of the propagation along the channel the following 1D Schrödinger equation:

$$\hat{H}\psi(\ell) = E\psi(\ell), \tag{A14}$$

where

$$\hat{H} = \begin{pmatrix} E_0 - \frac{\hbar^2}{2m_{\text{eff}}}\frac{d^2}{d\ell^2} + \frac{\Delta_z}{2} & \Omega_- - \beta\tau_- \frac{d}{d\ell}\tau_- \frac{d}{d\ell} \\ \Omega_+ - \beta\tau_+ \frac{d}{d\ell}\tau_+ \frac{d}{d\ell} & E_0 - \frac{\hbar^2}{2m_{\text{eff}}}\frac{d^2}{d\ell^2} - \frac{\Delta_z}{2} \end{pmatrix}, \tag{A15}$$

and we have used that

$$\int_{-\infty}^{+\infty} \phi(n)\frac{d\phi}{dn}\,dn = 0 \tag{A16}$$

and

$$E_0 = \int_{-\infty}^{+\infty} \phi(n)\left(-\frac{\hbar^2}{2m_{\text{eff}}}\frac{d^2}{dn^2} + U(n)\right)\phi(n)dn \tag{A17}$$

is the energy of the confinement, and

$$\Omega_\pm = \beta\tau_\pm^2 \int_{-\infty}^{+\infty} \phi(n)\frac{d^2\phi}{dn^2}dn \approx \frac{\beta}{d^2}\tau_\pm^2 = \Omega_0\tau_\pm^2, \tag{A18}$$

where $d$ is an effective width of the confining channel and we used Gaussion approximation, $\phi(n) = d\sqrt{\pi}\,e^{-n^2/(2d^2)}$.

Note that $E_0$ is just a constant, which can be safely dropped. As for the off-diagonal terms $\beta\tau_\pm\frac{d}{d\ell}\tau_\pm\frac{d}{d\ell}$, one can note that by the order of magnitude $d/d\ell \sim k$, where $k$ is a wave number, describing the propagation of the polaritons along the waveguide. Therefore, for narrow waveguides and small $k$, when $k \ll d^{-1}$, these terms can be neglected as compared to $\Omega_\pm$ and one gets the Hamiltonian (4) of the main text.


[1] I. Carusotto and C. Ciuti, Rev. Mod. Phys. **85**, 299 (2013).

[2] D. Ballarini, D. Caputo, C. S. Muñoz, M. De Giorgi, L. Dominici, M. H. Szymańska, K. West, L. N. Pfeiffer, G. Gigli, F. P. Laussy *et al.*, Phys. Rev. Lett. **118**, 215301 (2017).

[3] M. M. Glazov, H. Ouerdane, L. Pilozzi, G. Malpuech, A. V. Kavokin, and A. D'Andrea, Phys. Rev. B **80**, 155306 (2009).

[4] M. Vladimirova, S. Cronenberger, D. Scalbert, K. V. Kavokin, A. Miard, A. Lemaître, J. Bloch, D. Solnyshkov, G. Malpuech, and A. V. Kavokin, Phys. Rev. B **82**, 075301 (2010).

[5] E. Estrecho, T. Gao, N. Bobrovska, D. Comber-Todd, M. D. Fraser, M. Steger, K. West, L. N. Pfeiffer, J. Levinsen, M. M. Parish *et al.*, Phys. Rev. B **100**, 035306 (2019).

[6] C. Schneider, A. Rahimi-Iman, N. Y. Kim, J. Fischer, I. G. Savenko, M. Amthor, M. Lermer, A. Wolf, L. Worschech, V. D. Kulakovskii *et al.*, Nature (London) **497**, 348 (2013).

[7] D. G. Suárez-Forero, F. Riminucci, V. Ardizzone, M. D. Giorgi, L. Dominici, F. Todisco, G. Lerario, L. N. Pfeiffer, G. Gigli, D. Ballarini *et al.*, Optica **7**, 1579 (2020).

[8] J. F. Gonzalez Marin, D. Unuchek, Z. Sun, C. Y. Cheon, F. Tagarelli, K. Watanabe, T. Taniguchi, and A. Kis, Nat. Commun. **13**, 4884 (2022).

[9] D. D. Solnyshkov, M. M. Glazov, I. A. Shelykh, A. V. Kavokin, E. L. Ivchenko, and G. Malpuech, Phys. Rev. B **78**, 165323 (2008).

[10] P. Walker, T. C. H. Liew, D. Sarkar, M. Durska, A. P. D. Love, M. S. Skolnick, J. S. Roberts, I. A. Shelykh, A. V. Kavokin, and D. N. Krizhanovskii, Phys. Rev. Lett. **106**, 257401 (2011).

[11] M. Król, R. Mirek, D. Stephan, K. Lekenta, J.-G. Rousset, W. Pacuski, A. V. Kavokin, M. Matuszewski, J. Szczytko, and B. Pietka, Phys. Rev. B **99**, 115318 (2019).

[12] I. Shelykh, A. Kavokin, Y. Rubo, T. Liew, and G. Malpuech, Semicond. Sci. Technol. **25**, 013001 (2010).

[13] C. Ciuti, V. Savona, C. Piermarocchi, A. Quattropani, and P. Schwendimann, Phys. Rev. B **58**, 7926 (1998).

[14] D. Bajoni, P. Senellart, E. Wertz, I. Sagnes, A. Miard, A. Lemaître, and J. Bloch, Phys. Rev. Lett. **100**, 047401 (2008).

[15] G. Ctistis, A. Hartsuiker, E. van der Pol, J. Claudon, W. L. Vos, and J.-M. Gérard, Phys. Rev. B **82**, 195330 (2010).

[16] L. Ferrier, E. Wertz, R. Johne, D. D. Solnyshkov, P. Senellart, I. Sagnes, A. Lemaître, G. Malpuech, and J. Bloch, Phys. Rev. Lett. **106**, 126401 (2011).

[17] B. Real, N. Carlon Zambon, P. St-Jean, I. Sagnes, A. Lemaître, L. Le Gratiet, A. Harouri, S. Ravets, J. Bloch, and A. Amo, Phys. Rev. Res. **3**, 043161 (2021).

[18] M. Galbiati, L. Ferrier, D. D. Solnyshkov, D. Tanese, E. Wertz, A. Amo, M. Abbarchi, P. Senellart, I. Sagnes, A. Lemaître *et al.*, Phys. Rev. Lett. **108**, 126403 (2012).

[19] V. G. Sala, D. D. Solnyshkov, I. Carusotto, T. Jacqmin, A. Lemaître, H. Terças, A. Nalitov, M. Abbarchi, E. Galopin, I. Sagnes *et al.*, Phys. Rev. X **5**, 011034 (2015).

[20] M. Milićević, T. Ozawa, G. Montambaux, I. Carusotto, E. Galopin, A. Lemaître, L. Le Gratiet, I. Sagnes, J. Bloch, and A. Amo, Phys. Rev. Lett. **118**, 107403 (2017).

[21] H. Suchomel, S. Klembt, T. H. Harder, M. Klaas, O. A. Egorov, K. Winkler, M. Emmerling, R. Thomale, S. Höfling, and C. Schneider, Phys. Rev. Lett. **121**, 257402 (2018).

[22] C. E. Whittaker, E. Cancellieri, P. M. Walker, D. R. Gulevich, H. Schomerus, D. Vaitiekus, B. Royall, D. M. Whittaker, E. Clarke, I. V. Iorsh *et al.*, Phys. Rev. Lett. **120**, 097401 (2018).

[23] C. E. Whittaker, T. Dowling, A. V. Nalitov, A. V. Yulin, B. Royall, E. Clarke, M. S. Skolnick, I. A. Shelykh, and D. N. Krizhanovskii, Nat. Photon. **15**, 193 (2021).

[24] T. Kuriakose, P. M. Walker, T. Dowling, O. Kyriienko, I. A. Shelykh, P. St-Jean, N. Carlon Zambon, A. Lemaitre, I. Sagnes, L. Legratiet *et al.*, Nat. Photon. **16**, 566 (2022).

[25] D. D. Solnyshkov, G. Malpuech, P. St-Jean, S. Ravets, J. Bloch, and A. Amo, Opt. Mater. Express **11**, 1119 (2021).

[26] A. Gorbach, B. Malomed, and D. Skryabin, Phys. Lett. A **373**, 3024 (2009).

[27] D. Tanese, H. Flayac, D. Solnyshkov, A. Amo, A. Lemaître, E. Galopin, P. Braive, R. Senellart, I. Sagnes, G. Malpuech, and J. Bloch, Nat. Commun. **4**, 1749 (2013).

[28] E. A. Cerda-Méndez, D. Sarkar, D. N. Krizhanovskii, S. S. Gavrilov, K. Biermann, M. S. Skolnick, and P. V. Santos, Phys. Rev. Lett. **111**, 146401 (2013).

[29] E. A. Ostrovskaya, J. Abdullaev, M. D. Fraser, A. S. Desyatnikov, and Y. S. Kivshar, Phys. Rev. Lett. **110**, 170407 (2013).

[30] Y. V. Kartashov and D. V. Skryabin, Opt. Lett. **41**, 5043 (2016).

[31] D. A. Zezyulin, Y. V. Kartashov, and I. A. Shelykh, Phys. Rev. B **101**, 245305 (2020).

[32] Y. V. Kartashov and D. V. Skryabin, Optica **3**, 1228 (2016).

[33] M. Sich, J. K. Chana, O. A. Egorov, H. Sigurdsson, I. A. Shelykh, D. V. Skryabin, P. M. Walker, E. Clarke, B. Royall, M. S. Skolnick *et al.*, Phys. Rev. Lett. **120**, 167402 (2018).

[34] V. A. Lukoshkin, V. K. Kalevich, M. M. Afanasiev, K. V. Kavokin, Z. Hatzopoulos, P. G. Savvidis, E. S. Sedov, and A. V. Kavokin, Phys. Rev. B **97**, 195149 (2018).

[35] S. Mukherjee, D. M. Myers, R. G. Lena, B. Ozden, J. Beaumariage, Z. Sun, M. Steger, L. N. Pfeiffer, K. West, A. J. Daley *et al.*, Phys. Rev. B **100**, 245304 (2019).

[36] E. S. Sedov, V. A. Lukoshkin, V. K. Kalevich, P. G. Savvidis, and A. V. Kavokin, Phys. Rev. Res. **3**, 013072 (2021).

[37] K. Winkler, H. Flayac, S. Klembt, A. Schade, D. Nevinskiy, M. Kamp, C. Schneider, and S. Höfling, Phys. Rev. B **95**, 201302(R) (2017).

[38] J. Beierlein, E. Rozas, O. A. Egorov, M. Klaas, A. Yulin, H. Suchomel, T. H. Harder, M. Emmerling, M. D. Martín, I. A. Shelykh *et al.*, Phys. Rev. Lett. **126**, 075302 (2021).

[39] T. C. H. Liew, A. V. Kavokin, T. Ostatnický, M. Kaliteevski, I. A. Shelykh, and R. A. Abram, Phys. Rev. B **82**, 033302 (2010).
[40] T. C. H. Liew, I. A. Shelykh, and G. Malpuech, Phys. E **43**, 1543 (2011).
[41] F. Chen, H. Li, H. Zhou, S. Luo, Z. Sun, Z. Ye, F. Sun, J. Wang, Y. Zheng, X. Chen *et al.*, Phys. Rev. Lett. **129**, 057402 (2022).
[42] Y. Xue, I. Chestnov, E. Sedov, E. Kiktenko, A. K. Fedorov, S. Schumacher, X. Ma, and A. Kavokin, Phys. Rev. Res. **3**, 013099 (2021).
[43] D. Nigro, V. D'Ambrosio, D. Sanvitto, and D. Gerace, Commun. Phys. **5**, 34 (2022).
[44] I. A. Shelykh, A. V. Nalitov, and I. V. Iorsh, Phys. Rev. B **98**, 155428 (2018).
[45] H. Flayac, I. A. Shelykh, D. D. Solnyshkov, and G. Malpuech, Phys. Rev. B **81**, 045318 (2010).
[46] F. W. J. Olver, D. W. Lozier, R. F. Boisvert, and C. W. Clark, *The NIST Handbook of Mathematical Functions* (Cambridge University Press, Cambridge, UK, 2010).
[47] J. P. Boyd, Appl. Math. Comput. **218**, 7005 (2012).
[48] C. Wang, C. Gao, C.-M. Jian, and H. Zhai, Phys. Rev. Lett. **105**, 160403 (2010).
[49] T.-L. Ho and S. Zhang, Phys. Rev. Lett. **107**, 150403 (2011).
[50] Y. Li, L. P. Pitaevskii, and S. Stringari, Phys. Rev. Lett. **108**, 225301 (2012).
[51] V. Achilleos, D. J. Frantzeskakis, P. G. Kevrekidis, and D. E. Pelinovsky, Phys. Rev. Lett. **110**, 264101 (2013).
[52] Y. V. Kartashov, V. V. Konotop, and F. K. Abdullaev, Phys. Rev. Lett. **111**, 060402 (2013).
[53] M. Sich, D. N. Krizhanovskii, M. S. Skolnick, A. V. Gorbach, R. Hartley, E. A. Cérda-Mendez, K. Biermann, R. Hey, and P. V. Santos, Nat. Photon. **6**, 50 (2012).
[54] D. A. Zezyulin, Y. V. Kartashov, D. V. Skryabin, and I. A. Shelykh, ACS Photon. **5**, 3634 (2018).
[55] P. J. Y. Louis, E. A. Ostrovskaya, C. M. Savage, and Y. S. Kivshar, Phys. Rev. A **67**, 013602 (2003).
[56] N. K. Efremidis and D. N. Christodoulides, Phys. Rev. A **67**, 063608 (2003).
[57] D. E. Pelinovsky, A. A. Sukhorukov, and Y. S. Kivshar, Phys. Rev. E **70**, 036618 (2004).
[58] P. P. Kizin, D. A. Zezyulin, and G. L. Alfimov, Physica D **337**, 58 (2016).